Intl J Engg Sci Adv Research 2015 Sep;1(3): 188-193

Enhancing the performance of combined Wind, PV and Fuel hybrid generating systems

Ruchi Mishra
Department of Electrical Engg.
Rama University, Kanpur, India
tripathiruchi20@gmail.com

Gaurav Mishra
Department of Electrical Engg.
M.P.E.C., Kanpur,India
gaurav7859@gmail.com

Abstract: In recent years, solar and wind generating systems have advanced rapidly. Due to the intermittent nature of both the wind and photovoltaic energy sources, a fuel cell unit is added to the system for the purpose of ensuring continuous power flow. The fuel cell is thus controlled to provide the deficit power when the combined wind and photovoltaic sources cannot meet the net power demand. In this paper a hybrid energy system combining variable speed wind turbine, solar photovoltaic and fuel cell generation systems is presented to supply continuous power to residential power applications as stand-alone loads. The wind and photovoltaic systems are used as main energy sources while the fuel cell is used as secondary or back-up energy source. The maximum power is extracted from the wind turbine and the solar photovoltaic systems. The results show that even when the sun and wind are not available; the system is reliable and it can supply high quality power to the load.

Keywords: Hybrid energy system, variable speed wind turbine, photovoltaic array, fuel cell, step-up dc-dc converter, maximum power point tracking.

I. INTRODUCTION

Many renewable energy sources like wind turbine (WT) and solar photovoltaic (PV), which are clean and abundantly available in nature, are now well developed, cost effective and are being widely used, while some others like fuel cells (FC) are in their advanced developmental stage [1-4] . PV and WT have become two of the most promising sources of energy due to the fact that their energy sources are free and sustainable. Besides this, these energy sources are preferred for being environmental friendly.

The common inherent drawback of wind and photovoltaic systems are their intermittent natures that make them unreliable.

The integration of renewable energy sources to form a hybrid system is an excellent option for distributed energy production. In order to efficiently and economically utilize renewable energy resources of wind and PV applications, some form of back up is almost universally required. Storage energy systems as battery banks or super capacitors are very important for solar–wind power generation systems [5,6]. Solar and wind energy are stored during sunny and windy days and released later during cloudy days or at night, and to smooth power demands, electric energy is stored during off peak periods and later used during peak periods[7-10] .

Two dc–dc buck boost converters are employed for maximum power point tracking (MPPT) and dc output voltage regulation for each subsystem of PV and WT. Also, four complex fuzzy logic controllers (FLC) are designed to adjust the duty cycles of the two buck boost converters to achieve MPPT and output voltage regulation for wind and PV systems [11-13]. Proportional integrator (PI) type controller, which controls the duty cycle of the dc–dc converters.

This paper is aimed at combining WT, PV and FC generating systems to maximizing the output energy and reducing the output power fluctuations. The WT and PV are used as primary energy sources, while the FC is used as secondary or back-up energy source. Each system is combined with its individual dc–dc boost converter to control each of the three sources independently. The controller of WT and PV has the function of maximum power point tracking (MPPT) control while the controller of FC has the function of load power fluctuation compensator. A simple control method tracks the MPP of the WT is proposed without measuring the wind speed, which is very useful for actual small size wind turbines. The same control principle is applied to track MPP of the PV system without sensing the irradiance level and temperature. The FC is thus controlled to provide the deficit power when the primary combined PV and WT energy sources cannot meet the net load power demand. In the complete absence of power from the WT and PV sources, the FC will operate at its rated power capacity.

A simple MPPT controller is employed to achieve MPPT for both PV and wind energies and to deliver this maximum power to a fixed dc voltage bus. The fixed voltage bus supplies the dc load, while the ac loads are fed through a PWM inverter. The dc voltage bus can be regulated using a PWM voltage source inverter. The excess generated power can feed a water electrolyzer used to generate hydrogen for supplying the fuel cell. The dc power required for hydrogen generation can be

supplied directly through the dc bus during surplus PV and wind power. The generated hydrogen can be stored in tanks to be utilized by the fuel cells when the PV and wind energy sources fail to supply the load demand [14, 15].

II. HYBRID ENERGY SYSTEM CONFIGURATION

The system studied in this paper comprises of a 1 kW wind turbine generator, 1 kW solar photovoltaic and 1.25 kW fuel cell stack. The individual dc–dc converters in turn connected in parallel. The complete hybrid system is simulated for different operating conditions of the energy source. The simulation results prove the operating principle, feasibility and reliability of this proposed system. Fig. 2 illustrates the proposed hybrid energy system configuration composed of a PV, WT coupled to a PM generator with a three-phase diode bridge rectifier as primary energy sources and FC stack as back up energy source. All the three energy systems are connected in parallel to a common dc bus line through three individual dc–dc boost converters. The diodes D1, D2 and D3 play an important role in the system. The diodes allow only unidirectional current flow from the sources to the dc bus line, thus keeping each source from acting as a load on each other. Therefore in the event of malfunctioning of any of the sources, the respective diode will automatically disconnect that source from the overall system.

A. Solar photovoltaic

The building block of PV arrays is the solar cell, which is basically a p–n semiconductor junction. The current–voltage (I – V) characteristic of a solar photovoltaic is given by Equations given below [16-18]

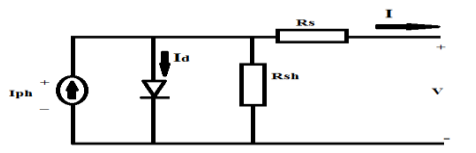

Fig. 1 Equivalent Circuit of PV cell

From the Equivalent circuit of PV cell-

$$I = I_{ph} - I_d \quad (1)$$

$$I = I_{ph} - I_o\left[exp\frac{q(V+R_s)}{Ak_BT} - 1\right] - \left(\frac{V+R_s}{R_{sh}}\right) \quad (2)$$

Where,
I_{ph} = Photocurrent, I_d = Diode current,
I_o= Saturation current, A = Ideality factor,
q = Electronic charge ($1.6x10^{-9}$C),
k_B= Boltzmann's gas constant ($1.38x10^{-23}$),
T = Cell temperature, R_s= Series resistance,
R_{sh}= Shunt resistance, I = cell current,
V = cell voltage

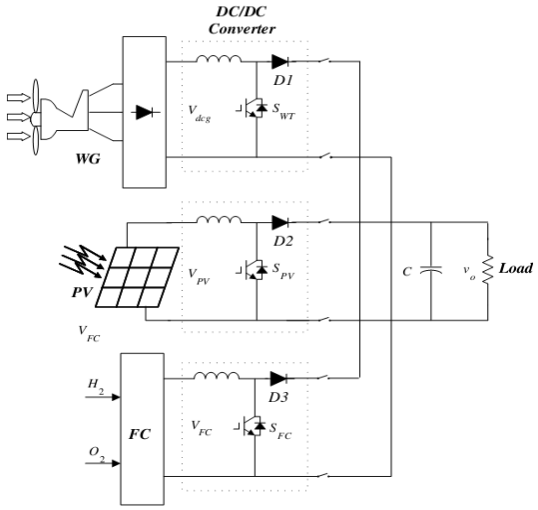

Fig.2 Proposed Hybrid Generating System

The output characteristics of a solar array as that shown in the experimental measurements of Fig. 3.

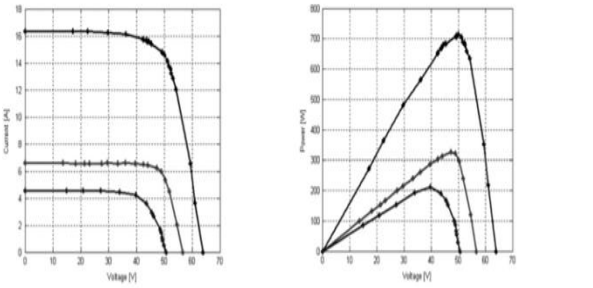

(a) I-V characteristics (b) P-V characteristics

Fig.3 Characteristics of PV Array

The I-V and P–V curves clearly show that the output characteristics of a solar PV are non-linear and are crucially influenced by the solar radiation, temperature and load condition [19].

Power output of the PV is given by [20]:

$$P_{PV} = I_{PV}V_{PV} \quad (3)$$

B. Wind turbine generator

The fundamental equation governing the mechanical power capture of the wind turbine rotor blades, which drives the electrical PM generator, is given by [21]

$$P = \frac{1}{2}\rho A C_P V^3 \quad (4)$$

where ρ is the air density(kg/m3), A is the area swept by the rotor blades, V is the air velocity (m/s), Cp represents the power coefficient of the wind turbine. Therefore, if the air density, swept area and wind speed are assumed constant the output power of the wind turbine will be a function of the power coefficient. The wind turbine is normally characterized by its Cp –TSR characteristic, where the TSR is the tip-speed ratio and is given by [22]:

$$TSR = \frac{\omega_m R}{V} \quad (5)$$

In Eq. (5), R and ωm are the turbine radius and the mechanical angular speed, respectively and V is the wind speed. The power coefficient has its maximum value at the optimal value of the tip-speed ratio (TSR opt) which results in optimum efficiency of the wind turbine and capture of maximum available wind power by the turbine.

C. Fuel cell system

The cell is an electrochemical device that generates electricity by a chemical reaction that does not alter the electrodes and the electrolyte materials. Thus, the fuel cell is a static device that converts the chemical energy of fuel directly into electric energy [23,24].

Water and heat are only the byproducts of the fuel cell if the fuel is pure hydrogen. The superior reliability, with no moving parts, is the additional benefit of the fuel cell as compared to the diesel generator [25].

Proton exchange membrane fuel cell (PEMFC) is the most promising fuel cell for small-scale applications. The PEM uses a polymer membrane as its electrolyte [26-29]. In the proposed system, air is used as the oxidant and hydrogen from a hydrogen tank as a fuel; the cell pressure is atmospheric and the cell temperature is 70 °C.

PEMFCs are gaining importance in many applications as distribution systems because of their low operating temperature, higher power density, specific power, longevity, efficiency, relatively high durability and the ability to rapidly adjust to changes in power demand. Furthermore, PEM fuel cells have the advantage that they can be placed at any site in a distribution system, without geo-graphic limitations, to achieve the best performance [30,31].

The net reaction in a typical FC is given by

$$2H_2 + O_2 \rightarrow 2H_2O \quad (6)$$

The output of the fuel cell is given by

$$V_{FC} = E_{Nernst} - V_{Act} - V_{Ohmic} - V_{Con} \quad (7)$$

where:

E_{Nernst}: Thermodynamic potential of the cell representing its reversible voltage.
V_{Act}: Voltage drop due to the activation of the anode and cathode. It is a measure of the voltage drop associated with the electrodes.
V_{Ohmic}: Ohmic voltage drop resulting from the resistances of the conduction of protons through the solid electrolyte and the electrons through its path.
V_{Con}: Voltage drop resulting from the reduction in concentration of the reactants gases or, alternatively, from the transport of mass of oxygen and hydrogen.

The instantaneous electric power of each fuel cell is given by equations 8 [10]:

$$P_{FC} = V_{FC} \times i_{FC} \quad (8)$$

where:

i_{FC}: Cell operating current (A),
V_{FC}: Output voltage of the fuel cell for a given operating condition (V),
P_{FC}: Output power of each fuel cell (W).

III. System Control

As shown in Fig. 2, dc-dc boost converter divides the system voltage into two levels, variable voltage at the output terminal of the energy source Vi and fixed dc voltage at the dc bus line (load terminal) Vo .

The state equations of dc-dc boost converter can be given by (9), where S is the switch state that takes the value 1or 0, Vi is the input voltage to the dc-dc converter output from each energy source) and Vo is the dc link output voltage.

(9)

In PV and WT systems, the terminal voltage is controlled based on the voltage error signal. For the PV system, the PV

voltage and current are sensed to determine the reference voltage at which MPP occurs. The error signal which is the difference between the reference voltage and the actual voltage of the PV is fed to the voltage controller to control the duty cycle of the PV boost converter. For the WT the error signal is the difference between the reference rectified voltage of the PMG for MPPT and measured rectified voltage. This error signal is fed to the voltage controller which controls the duty cycle of the WT boost converter.

The total supply generated power must be controlled so as to meet the required load demand since the output power of photovoltaic and wind turbine generators fluctuate with irradiation and wind speed. The FC output power is controlled based on the difference power command ΔP, which is the load power (command value) PS minus the summation of the power generated from the PV and WT PPV and PWT, respectively,

$$P_{FC} = \Delta P = P_S - P_{PV} - P_{WT} \quad (10)$$

Fig. 4 shows the configuration of control topology of the three individual dc-dc converters. Since this system cannot allow reverse power flow, because of the configuration of dc boost converter, many generating units can be connected in parallel.

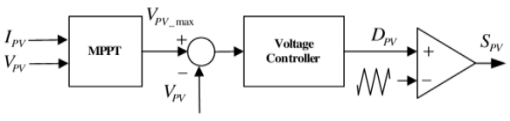

(a)MPPT of photovoltaic system

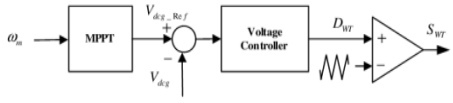

(b) MPPT of Wind Turbine system

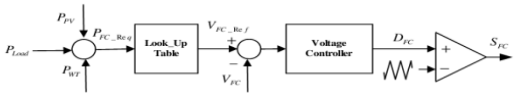

(c) Fuel cell stack

Fig. 4 Control principles of dc-dc boost converters

IV. SIMULATION RESULTS

Power module fuel cell stack consists of 50 cells connected in series to produce rated output power of 1.25 kW. The hybrid system is sized to power a typical 2kW/150 V dc telecommunication load or an ac residential power application continuously through the year in remote locations or isolated islands. The load is simulated as a constant resistive load connected to a fixed dc bus line voltage,

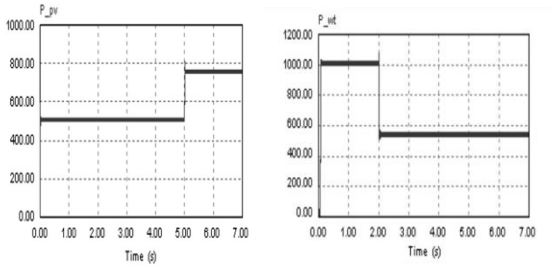

(a) PV output power (b) WT output power

Fig. 5 variation of the power output of the energy sources

Fig. 5 a shows the PV system is assumed to be 0.5 kW initially and then increases to 0.75 kW due to a sudden increase of irradiance level from 0.7 to 1.0 kW/m at 0.5 s.

Fig. 5b indicates that the WT output is generating 1.0 kW initially and then decreases to 0.5 kW due to a sudden decrease in wind speed from 15.6 to 2.5 m/s at 0.2 s.

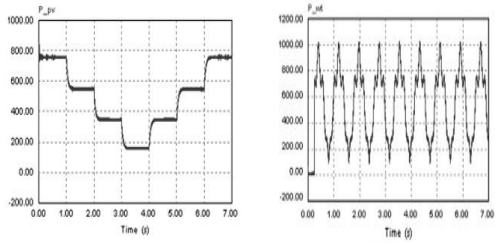

(a)PV output power (b) WT output power

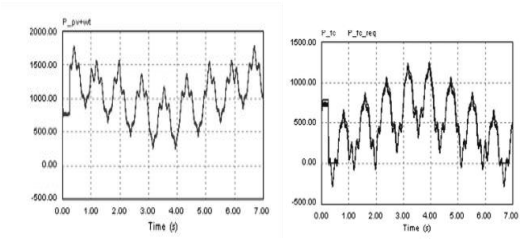

(c) Simulation of PV & WT (d) FC command power & generated power output power

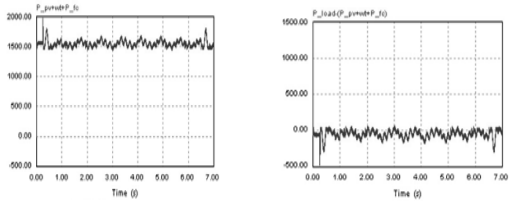

IV. SIMULATION RESULTS

(e) Hybrid system output power (f) error in supply power demand

Fig.6 Generated power in PV, WT & FC and total output power

It is clear in both cases of Fig. 6 a and b that the curves of maximum available PV and wind power coincide with the generated output power, which proves that the controller forces the system to extract the maximum power and deliver it as useful electric energy to the dc-link bus.

The reference power command of FC is determined as the difference between the load power 2.0 kW and the generated power of PV and WT. The output power of the FC system is shown in Fig. 6c, which varies with the changes in the PV and WT output power. The FC output power changes from 0.5 kW to 1.0 kW and then to 0.75 kW at a time of 0.2 and 0.5 s, respectively. Fig. 6 d indicates the total generated power of the hybrid system. From Fig. 6 d, it is clear to note that the hybrid system output power is always maintained constant at the load power demand in spite of the fluctuations in the PV and WT output power.

Fig. 7 proves the concept of individual control of dc–dc converters of the three sources.

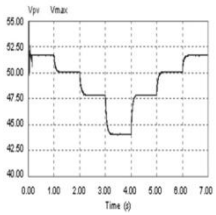

(a) Ref. (V_{mp}) & output voltage of PV system

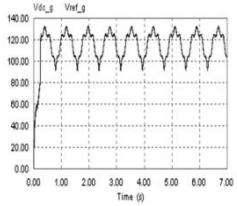

(b) Ref. (V_{dcg_ref}) & PMG rectified voltage

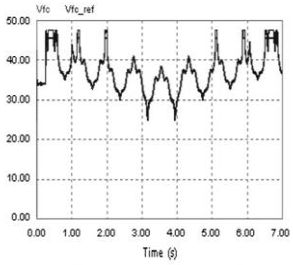

(c) Reference and output voltage of FC

Fig.7 Control of PV, WT and FC systems

From Fig. 7 a, it is clear that the PV output voltage follows well the reference voltage of the maximum power point to extract the maximum power of the PV system. Fig. 7 b shows the effective control of the PM generator rectified voltage follows the reference value to track the maximum power of WT. Detailed results of both PV and WT systems as the controller duty cycles for MPPT and output voltages can be found in [22]. Finally, Fig. 7 c shows the output voltage control of the FC, which coincides well with the reference voltage from the controller (FC required power), to generate the deficit power between the load demand and the generated power from the PV and WT systems.

Fig. 7a plots the variation in PV output power as the insulation changes rapidly and continuously. Fig. 7b shows the output power variation of WT as the wind speed changes rapidly and continuously. Detailed change in the insulation and wind speed changes are listed in [21] . Summation of PV and WT outputs is shown in Fig. 7 c.

Fig. 8 shows the efficient control of the three dc–dc converters to control the reference output voltage of the three systems to track its reference value even under sudden and continuous change in the irradiance level and wind speed.

Fig. 8 illustrates the changes in output voltage, stack current and airflow that accompany a step change in load for Nexa Barrad FC. At idle, the oxidant airflow rate closely tracks the requested flow. After a load step to full power, the air pump rapidly speeds up. There is a brief (about 0.5 s) undershoot (2.5 V) in stack voltage during this transient, before the output voltage stabilizes at 26 V. Stack current also increases slightly during this transient interval, due to increased parasitic power draw from the air compressor. A similar transient interval occurs after a load step from full power to idle. Airflow is gradually reduced, due to inertia in the air pump.

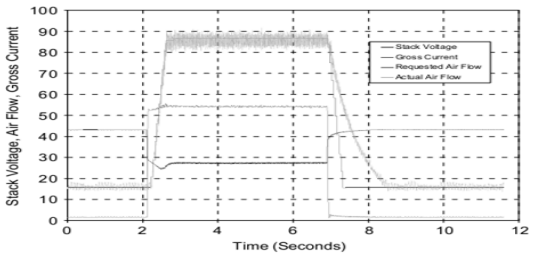

Fig.8 Nexa Barrad PEMFC transient response characteristic

Output voltage gradually recovers and stabilizes to 43 V over a 0.5 s interval. Therefore, the Nexa Ballard FC has a fast dynamic response; it takes only 0.5 s to accelerate from no load to its rated output power. Also, it can reduce its output from rated power to idle at 0.5 s. Therefore, it is able to suppress most of the fluctuations in the output power of PV and WT hybrid system up to 2 Hz. High frequency fluctuations can be suppressed using storage devices as electrolytic double layer capacitor (EDLC), which is the subject of future work. Such device is necessary to suppress the high frequency fluctuations

for very critical loads and to absorb the excessive generated power. Therefore, the system can supply very high-quality power to load demand.

V. CONCLUSIONS

The output power of wind turbine and solar photovoltaic generators mostly fluctuates and has an effect on system frequency. One of the existing methods to solve these issues is to install batteries which absorb power from wind turbine generators. The other method is to install dump loads which dissipates fluctuating power. However, such methods are costly and not effective and cannot guarantee continuous power flow to the load. Therefore, this paper presents a solar photovoltaic, wind turbine and fuel cell hybrid generation system to supply a continuous output power. The fuel cell is used to suppress the fluctuations of the photovoltaic and wind turbine output power. The photovoltaic and wind turbines are controlled to track the maximum power point at all operating conditions. The fuel cell is controlled to supply the deficit power between the load power demand and the generated power of the combined photovoltaic and wind turbine sources. Therefore, the proposed hybrid generation system can supply high-quality power.

REFERENCES

[1] Rubbia Carlo. Today the world of tomorrow—the energy challenge. J Energy Convers Manage 2006;47(17):2695–7.

[2] Hamada Y, Goto R, Nakamura M, Kubota H, Ochifuji K.Operating results and simulations on a fuel cell for residential energy sys. J Energy Convers Manage 2006;47(20):3562–71.

[3] Hamada Y, Nakamura M, Kubota H, Ochifuji K, Murase M, Goto R. Field performance of a polymer electrolyte fuel cell for a residential energy system. Renew Sust Energy Rev 2005;9(4):345–62.

[4] Kim YH, Kim SS. An electrical modeling and fuzzy logic control of a fuel cell generation system. IEEE Trans Energy Convers 1999;14(2):239–44.

[5] Dokopoulos PS, Saramourtsis AC, Bakirtzis AG. Prediction and evaluation of the performance of wind-diesel energy systems. IEEE Trans Energy Convers 1996;11(2):385–93.

[6] Zahran Mohamed BA. Photovoltaic hybrid systems reliability and availability. Int J Power Electron 2003;3(3):145–50.

[7] Ackermann T, Soder L. An overview of wind energy—status 2002. Renew Sust Energy Rev 2002;6(1–1):67–128.

[8] Ozgener Onder. A small wind turbine system (SWTS) application and its performance analysis. J Energy Convers Manage 2006;47(11–12):1326–37.

[9] Wang P, Billinton R. Reliability benefit analysis of adding WTG to a distribution system. IEEE Trans Energy Convers 2001;16(2):134–9.

[10] Tian W, Wang Y, Ren J, Zhu L. Effect of urban climate on building integrated photovoltaics performance. J Energy Convers Manage 2007;48(1):1–8.

[11] Bose BK, Szczeny PM, Steigerwald RL. Microcomputer control of a residential photovoltaic power conditioning system. IEEE Trans Ind Electron 1985;IA 21 (Sept/Oct):1182–91.

[12] Jiang JA, Huang TL, Hsiao YT, Chen CH. Maximum power tracking for photovoltaic power systems. Tamkang J Sci Eng2005;8(2):147–53.

[13] Hussion KH, Zhao G. Maximum photovoltaic power tracking: an algorithm for rapidly changing atmospheric conditions. Proc IEE 1995;142(1):59–64.

[14] Hua C, Lin J, Shen C. Implementation of a DSP controlled photovoltaic system with peak power tracking. IEEE Trans Ind Electron 1998;45(1):99–107.

[15] Mitchell K, Nagria M, Rizk J. Simulation and optimization of renewable energy systems. J Elect Power Energy Syst2005;27(3):177–88.

[16] Yang Hongxing, Lu Lin, Zhou Wei. A novel optimization sizing model for hybrid solar–wind power generation system. J Sol Energy 2007;81(1):76–84.

[17] Hoff Thomas E, Perez Richard, Margolis Robert M.Maximizing the value of customer-sited PV systems using storage and controls. J Sol Energy 2007;81(7):940–5.

[18] Ayad Mohamed-Yacine, Pierfederici Serge, Rael Stephane, Davat Bernard. Voltage regulated hybrid DC power source using supercapacitors as energy storage device. J Energy Convers Manage 2007;48(7):2196–202.

[19] Billinton Roy, Karki Rajesh. Capacity expansion of small isolated power systems using PV and wind energy. IEEE Trans Power Syst 2001;6(4):892–7.

[20] Karki RajeshRajesh, Billinton Roy. Reliability/cost implications of PV and wind energy utilization in small isolated power systems. IEEE Trans Energy Convers 2001;16(4):368–73.

[21] Celik Ali Naci. Techno-economic analysis of autonomous PV–wind hybrid energy systems using different sizing methods. J Energy Convers Manage 2003;44(12):1951–68.

[22] Rajashekara Kaushik. Hybrid fuel-cell strategies for clean power generation. IEEE Trans Ind Appl 2005;41(3):682–9.

[23] Sekiguchi N, Tani T. Fundamental study onphotovoltaic/fuel cell power hybrid system (characteristic of system utilized hydrogen absorbing alloys). Trans Inst Elect Eng IEEJ 1997;117-B(3):402–8.

[24] Islam Saiful, Belmans Ronnie. Grid independent photovoltaic fuel-cell hybrid system: design and control strategy. KIEEInt Trans Elect Mach Energy Convers Syst 2005;5-B(4):399–404.

[25] Senjyu Tomonobu, Nakaji Toshiaki, Uezato Katsumi, Funabashi Toshihisa. A hybrid power system using alternative energy facilities in isolated island. IEEE Trans Energy Convers 2005;20(2):406–14.

[26] El-Shatter Thanaa F, Eskander Mona N, El-Hagry Mohsen T.Energy flow and management of a hybrid wind/PV/fuel cell generation system. J Energy Convers Manage 2006;47(9–10):264–1280.

[27] Powersim Technologies. PSIM version 7.1, for power electronics simulations. User manual. Powersim Technologies, Vancouver, Canada.

[28] http://www. powersimtech.com .

[29] Uzunoglu M, Alam MS. Dynamic Modeling, Design and simulation of a PEM fuel cell/ultra-capacitor hybrid system for vehicular applications. J Energy Convers Manage 2007;48(5):1544–53.

[30] Ahmed Nabil A. Computational modeling and polarization characteristics of proton exchange membrane fuel cell with evaluation of the interface systems. Eur Power Electron J,EPE 2008;18(1): in press. N.A.